A Cellular Automaton Model of Laser-Plasma Interactions

D. Batani

Dipartimento di Fisica "G. Occhialini", Università di Milano-Bicocca,
INFM, Unità di Milano-Bicocca
via Emanueli, 15 20126 Milano, Italy
batani@mi.infn.it

S. Biava, S. Bittanti, F. Previdi

Dipartimento di Elettronica & Informazione, Politecnico di Milano
via G. Ponzio 34/5 20133 Milano, Italy
{bittanti,previdi}@elet.polimi.it

Keywords: Cellular Automata, Laser-Plasma Interaction, Physical-Based Modelling

Abstract

This paper deals with the realization of a CA model of the physical interactions occurring when high power laser pulses are focused on plasma targets. The low-level and microscopic physical laws of interactions among the plasma and the photons in the pulse are described. In particular, electron-electron interaction via the Coulomb force and photon-electron interaction due to ponderomotive forces are considered. Moreover, the dependence on time and space of the index of refraction is taken into account, as a consequence of electron motion in the plasma. Ions are considered still particles and the main effect of their presence is the range reduction of the Coulomb force. Simulations of these interactions are provided in different conditions and the macroscopic dynamics of the system, in agreement with the experimental behaviour, are evidenced.

1 Introduction

The recent advent of femtosecond lasers [1] has opened new perspectives in the research on laser produced plasmas. In particular, important new results have been obtained in the field of *soft X-ray lasers* [2]. Among other works, it is worth noting the progresses in high order harmonics generation and its applications [3]; sources of relativistic particles [4]; laser acceleration of electrons [5]; highly non linear interactions and laser beam self-focusing [6,7]; and the new "fast ignitor" approach to Inertial Confinement Fusion (ICF) [8]. Sophisticated computer codes are already available to simulate plasmas produced by such short laser pulses, including Particle-In-Cell (PIC) codes [9], Vlasov codes [10,11] and Fokker-Planck codes [12].

In this paper, a Cellular Automaton (CA) model of laser-plasma interaction will be presented. In particular, the interaction between a short laser pulse and a fully ionized plasma will be considered.

The development of simulation tools based on Cellular Automata appears very interesting for a number of reasons. First of all, CA codes allow a direct representation of low-level elementary physical laws, the complex macroscopic dynamics of the global system emerging from "simple" microscopic interaction rules among the cells of the CA. In some situations, this may allow a better understanding on the ongoing physics (see [13-19]. Moreover, in general, in the experimental protocols, the laser generates very short pulses ($\tau \cong 100$ fs) which are focused on a small focal spot ($d \cong 10$ μm) in order to obtain the high intensity necessary to create and study the plasma. The transversal dimension of the region filled with the plasma is of the order of the focal spot size; the longitudinal dimension is of the order of the focal depth of the lens ($L \cong 100$ μm). So, the physical phenomena that are the subject of the simulation are confined in a very small region of space and takes place in a very short time. Thus, it is possible to conceive a CA code that performs a 1:1 simulation of the laser-plasma interaction dynamics. In other words, CA allow the simulation of the "true" dynamical evolution of the system with a very high temporal and spatial resolution.

Basically, CA may be used in two different ways: as computational tools, for solving differential equations (used together with parallel computers) [20] or as a dynamical systems completely discrete (both in time and state variables) used as a physical-based model [13,18,21,22]. In this work the second approach is followed, using a cellular automaton to describe the radiation-matter interaction between a laser pulse crossing a hot plasma.

CA have already been used for direct physical-based modelling of systems. In particular, applications can be found in biology for DNA sequences modeling [23] and cytoskeleton formation modeling [24]; in vulcanology to simulate lava streams [25]; for bioremediation of contamined soils [26]; in fluidodynamics, for turbulence simulation [14]; in chemistry, for the investigation of crystal growth dynamics [27]; in optoelectronics, for simulation of the behaviour of semiconductor integrated optical devices [18,22].

The paper has the following structure: in Sect. 2 a presentation is given of the CA as discrete (in time and state variables) dynamical systems. In Sect. 3 the basic physical laws of laser-plasma interaction are introduced. Sect. 4 is devoted to the outline of the CA implementation of the physics described in the previous section. Section 5 contains the simulation results presented following a step by step procedure, i.e. by separately presenting the effects of each single interaction and, finally, by merging all the rules of evolution in a single CA model.

2 Cellular Automata as discrete dynamical systems

Cellular Automata are discrete time dynamical system made by many identical and simple interconnected subsystems, called *cells*. Each cell interacts with a finite number of other cells, i.e. those belonging to a user-defined *neighbourhood*. The interaction among each cell and its neighbourhood is governed by suitable set of *rules of evolution*. A number of *state variables* can be defined as function of space (through the cell position in the CA) and time. So, a CA model is fully defined by the following items:

- the *cellular space*, which is a discrete lattice of spatially distributed cells;
- the *state variables* defined for each cell;
- the *neighbourhood of a cell*, i.e. the ensemble of all the cells that must be examined to determine the state of the considered cell;
- the *evolution rules*, also called dynamic equations of the system. They are local in space and time, i.e. their value depends only on the value of the state of a neighbourhood of cells for a fixed number of previous time steps (usually one).

The properties of uniformity, locality and discreteness that define CA make them suitable to reproduce the behaviour of complex dynamic systems, characterized by discrete elements with local (usually nonlinear) interactions. So, CA may be considered as an alternative to differential/difference equations in building and computing mathematical models of nature, as they are capable to describe systems with a great number of degrees of freedom.

3 Basic Physics of Laser-Plasma Interactions

In this section we give a brief overview of the properties of a plasma and of the interactions which take place inside it. The goal is both to give some basics notions for non-specialists regarding the physics we want to simulate, and to give a basis for the implementation of the interaction rules (i.e. the CA evolution laws) described in next section.

Plasma is a material in which the majority of the atoms and molecules are dissociated in positive ions and electrons. In fact, even if on earth there are a few examples of plasmas (apart from plasmas generated in laboratory, we may recall bolts and aurora borealis), in the universe more than 99% of matter is in the state of plasma, i.e. ionised.

In our case we refer to plasmas which are generated by the interaction of a short-pulse high-intensity laser with a gas. Even with such very fast lasers, a very high ionisation degree is achieved during the very first phases of the interaction, after which the laser interacts with the plasma. Hence, in our physical models and in the CA code which implements them, we will neglect the physics connected to ionisation of atoms and molecules in the gas which is only important at the beginning, and we will concentrate on later phases. However, it is worth noting that, including ionisation appears a rather easy task.

As already recalled in the introduction, the laser produces very short pulses ($\tau \cong 100$ fs) and is focused on a small focal spot ($d \cong 10\mu m$). The transverse dimension of such a plasma region is of the order of the focal spot size, and the longitudinal one is of the order of the lens focal depth ($L \cong 100\ \mu m$). Moreover, such small plasma volume ($V \cong 8\times10^{-9}$ cm^3 or 8000 μm^3) contains a huge number of molecules ($\cong 2\times10^{11}$ corresponding to a density $\cong 3\times10^{19}$ molecules/cm^3). Evidently such numbers only allow a representation of the physical system through statistical quantities. Hence the typical parameters usually used to represent the physical state of a plasma are:

- the electron density (n_e) and the ionic density (n_i) both usually expressed in cm^{-3}. Electric charge conservation implies that $n_e = Z^* n_i$ where Z^* is the average ionisation degree.
- the electron temperature (T_e) and the ion temperature (T_i) usually expressed in energy units (i.e. eV). The large mass difference between electrons and ions implies different inertia. This means that, while electrons are easily and quickly heated by the incident laser beam, ions react on a very different time scale. So, we may have $T_i = 0$ eV (or the initial, low, gas temperature) while T_e reaches several tents eV. On the other end at very late times thermal equilibrium implies $T_e = T_i$.

The propagation of a laser beam in the plasma is substantially different from that in vacuum or in an underdense gas. Indeed the dispersion relation is :

$$\nu^2 = \nu_p^2 + c^2 \Big/ \lambda^2 \qquad (1)$$

where c is the velocity of light, ν and λ are the laser frequency and wavelength and ν_p is the plasma frequency (whereas in vacuum we get the usual relation between wavelength and frequency $\nu\lambda=c$). The plasma frequency characterises the electron motion: a plasma at equilibrium is neutral, whenever a charge separation is generated, a strong electric field arises which moves the charged particles in order to restore the initial equilibrium conditions. This produces "plasma oscillations" characterized by a proper plasma frequency.

The presence of these plasma oscillations reflects in a dependence of the index of refraction of the plasma n on the electron density

$$n(x,y,z) = \left(1 - n_e(x,y,z) \Big/ n_c\right)^{\frac{1}{2}} \qquad (2)$$

that produces, as we will see in the following, a feedback effect is the core of the aspects we want to simulate. Here $n(x,y,z)$ and $n_e(x,y,z)$ are respectively the refractive index of the material and the electron density at the point (x,y,z), and n_c is the critical density, which represents the density value above which an electromagnetic wave cannot propagate in the plasma.

As already said, the laser pulse is characterised by a short duration ($\tau \cong 100$ fs), a tight focus ($d \cong 10\mu m$), a wavelength λ and an intensity I. In the following, we will assume that the distribution of laser intensity is characterised by a cylindrical symmetry and by a gaussian shape both in space and time:

$$I(r,t) = I_0 e^{-2.77\left(\left(\frac{r}{r_0}\right)^2 - \left(\frac{t}{\tau}\right)^2\right)} \qquad (3)$$

where r_0 and τ are the values corresponding to $I_0/2$ in space and time (i.e. half the FWHM values). Typically in the kind of experiments we want to simulate, we have I_0 at least of the order of 10^{17} W/cm^2 and $\lambda \cong 1$ μm (near infrared radiation). The photon energy is given by Planck relation as $E = h\nu = hc/\lambda$ and is $\cong 1$ eV. The total energy in the laser pulse is obtained by space and time integration of Eq. (3):

$$E_L = \int dt \int 2\pi r dr I_0 e^{-2.77\left(\left(\frac{r}{r_0}\right)^2 - \left(\frac{t}{\tau}\right)^2\right)} \cong 10\,\text{mJ} \qquad (4)$$

This corresponds to a number of photon in the pulse $\approx 6\times10^{16}$. As in the case of matter particles, we see that an individual representation of single photons is not possible and we turn to using a photon density n_{ph} (measured in cm^{-3}).

Also in the experimental set-up, a lens is used to focus the laser pulse to the small focal spot with diameter $d \cong 10$ μm so that the very high intensity quoted before can really be obtained. Usually the F number of the lens is of the order of 1/3 which means that the lens diameter is 1/3 of its focal length. This tight focus reflects in a short focal depth ($L \cong 100$ μm as previously quoted).

After describing the type of particles that play a role in laser-plasma interactions (electrons, ion, photons), we give a brief description of the basic interactions which take place between them. We make the further simplifying approximation of considering the positive ions as a fixed background as a consequence of their large inertia. Such assumption allows the system description to be reduced to electrons and photons. While it is generally valid in the initial stages of the interaction, this assumption may fall at later times not only in connection with the ionic time-scale, but also as a consequence of the huge electric fields which can be produced by the charge separation connected to electron displacement.

3.1 Electron-electron interactions

Electrons interact between them via the Coulomb electric field. Unlike in vacuum, in a plasma a screening effect due to the presence of the many charged particles must be taken into account. This reflects in the existence of an effective shielding distance (the Debye length).

3.2 Photon-electron interactions

Photons may act over the electrons by means of the *ponderomotive* forces. These are the results of radiation pressure and tend to move the electrons away from the regions where the intensity of electromagnetic field is higher. The force acting on a single electron is

$$F_p = -\frac{\nu_p^2}{nec\nu^2}\nabla I \qquad (5)$$

where I is the laser pulse intensity that can be alternatively expressed through the local instantaneous photon density.

3.3 Electron-photon interactions

Electrons act over the photons via the changes in the plasma local refractive index, as expressed by Eq. (2). The changes in n(x,y,z) induce both changes in the photon direction (in agreement with Snell's law) and in photon velocity. In our case the plasma has a density which is a factor of 100 smaller than n_c ($\cong 10^{21}$ cm^{-3} for a laser wavelength $\lambda \cong 1$ μm) so that the second effect is almost negligible.

3.4 Photon-photon interactions

Obviously photons do not interact with each other. However, we must consider that being fundamental particles they are subject to Heisemberg's principle. In our case this has important consequences: passing through the lens which focuses them, their position become determined within a dimension D (the diameter of the lens). This implies an uncertainty of the order of h/D (h being Planck's constant) in the momentum of the photon along the same direction, which reflects in the spatial spread of photons in the focal plane. This is the only way of introducing the departure from geometrical optics (which would imply a perfect focusing in a geometrical point and an infinite laser intensity in the focal point) in a purely particle context, as those treated by CA codes.

Apart from these interactions it must be considered that both electrons and ions are subject to a random motion (due to thermal agitation at the temperature T) and to a hydrodynamical pressure. This last can be treated analogously to the radiation pressure. Both these effects have been neglected in the present work because they are predicted to have a smaller influence with respect to the main interactions we have considered here.

Due to the photon-electron interactions and ponderomotive forces, when an electromagnetic field propagates in plasma, electrons are forced to move from the equilibrium position to the areas where the intensity of the field is smaller. The induced variation of the electron density creates a gradient of the refractive index that modifies the photon motion in the plasma (electron-photon interaction), diverting their original direction of motion. This creates an interaction loop characterised by a feedback mechanism, as evidenced in Sect. 5.5 (see also Fig. 8). Due to this effect, the laser may undergo focalisation in the plasma provided the laser power is bigger than a given critical power (self focusing effect) [6,7].

4 Cellular Automaton Implementation of Laser-Plasma Interactions

In this section the main features of the proposed model will be described. In the following, the practical implementation of each interaction introduced in Sect. 3 will be outlined. All the CA rules will be introduced on the same topological structure, i.e. the cellular space. In particular, a two-dimensional triangular lattice with hexagonal symmetry has been chosen. The cellular space represents a transversal section of the region filled with the plasma where the laser-plasma interaction will take place (see Fig. 1). Due to the propagation of radiation in the plasma, the dimension of a cell l and the discrete time step Δt must satisfy the following condition:

$$\frac{l}{c} = \Delta t \qquad (6)$$

where c is the speed of light in vacuum. The relationship (6) between the automaton spatial step l, i.e. the distance between two nearest cells of the lattice, and the discrete

time step Δt will be fulfilled in all the rules of evolution that will be used in this paper.

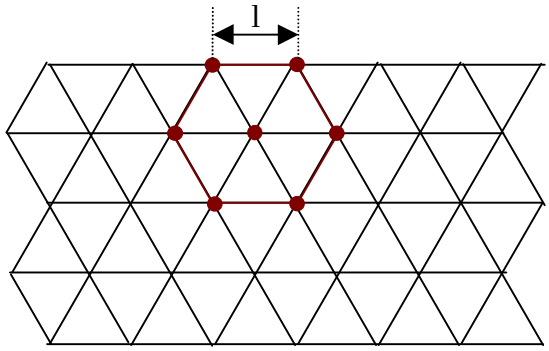

Figure 1: Cellular space with triangular geometry and hexagonal symmetry. The CA cells are placed on the vertex of the triangles. It is evidenced the classical hexagonal neighbourhood and the spatial size l.

Typically, we will choose a time step $\Delta t \cong 1$ fs that implies $l \cong 0.3$ μm. These values allow a sufficient resolution both in time ($\tau/\Delta t \cong 100$) and in space ($d/l \cong 33$).

The state variables of the model depend on both time and space, i.e. the cell position. In particular, the number of electrons at time k in the cell (i,j) will be denoted by $N_{el(k)}(i,j)$ and the number of photons for each direction of motion s will be indicated by $N^{s}_{ph(k)}(i,j)$. Then, the interactions described in Sect. 3 can be described by three different evolution rules.

Finally, we notice that the chosen topology for the cellular space is two-dimensional (although a three-dimensional model could be possibly considered in future), while the physical problem is a true three-dimensional one, even if with a cylindrical symmetry. However, a specific volume could be assigned to each single cell, i.e. that of the torus with the hexagonal cell as a basis, so that the photon and electron density can become a photon and electron number, in order to evaluate the forces.

4.1 Photon propagation

The laser pulse can be seen as a bunch of photons coming in the region filled with the plasma from one side (say the left) and outgoing from the opposite one (say the right). Hence, in order to describe correctly the propagation of photons, the neighbourhood of a cell (i,j) for this evolution rule will be taken non-symmetric. This is not strictly necessary, but leads to a computational simplification. In our CA code, we consider a realistic case of laser beam propagation. In particular, we forget the plane wave approximation (as done for instance in [18,21]) and we consider the case of a beam focused through a lens, converging down to a focal position and diverging again. Although apparently simple, this problem is difficult to be implemented with a CA. Indeed, it is necessary to settle the possible infinite directions of propagation for the photons on the cellular space, where only six directions are available, i.e. NO, NE, E, SE, SO, O (see Fig. 2).

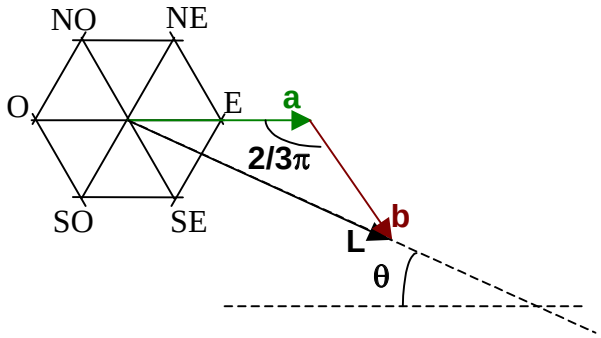

Figure 2: Example of the decomposition of the motion of a photon.

So, the neighbourhood of the cell (i,j) is defined by all the cells that lie along the possible directions of motion that end in the cell (i,j), i.e.

$$\mathcal{N}(i,j) = \left\{ (i^*, j^*), \text{so that the cell } (i,j) \text{ can be reached starting from } (i^*, j^*) \text{ and moving in the NE, SE, E directions} \right\} \quad (7)$$

Since it is not possible to manage an infinite number of direction, a quantization of the possible directions is performed, i.e. only a finite number s = 1,…,M is considered. In particular, the CA spatial steps and the focal length of the focusing lens fixes the number of possible initial directions of motion. Then, each of the possible directions is decomposed along the available directions of the cellular space. As an example, consider a photon moving of a distance L along a direction with angle between the E and SE directions (see Fig. 2). The following decomposition expression for the motion will be obtained:

$$a(i,j) = \frac{L \cdot \sin\left(\frac{\pi}{3} - \theta(i,j)\right)}{\sin\left(\frac{2}{3}\cdot\pi\right)}$$
$$b(i,j) = \frac{L \cdot \sin\left(\theta(i,j)\right)}{\sin\left(\frac{2}{3}\cdot\pi\right)} \quad (8)$$

Then, the number of discrete space steps n_E in the E direction and n_{SE} in the SE direction is computed by:

$$n_E = \left[\frac{a(i,j)}{l}\right] \text{ and } n_{SE} = \left[\frac{b(i,j)}{l}\right]$$

where $[\cdot]$ is the operator which takes the nearest integer of its argument.

The CA rule of evolution describing the motion of photons is the following:

$$N^{(s)}_{ph_{(k+1)}}(i,j) =$$

$$= \sum_{r=1}^{M} \sum_{(i^*,j^*)\in\mathcal{N}(i,j)} N^{(r)}_{ph_{(k)}}(i^*,j^*) \cdot R^{(r,s)}_{(k)}(i^*,j^*) \quad (9)$$

with

$$R_{(k)}^{(r,s)}(i^*, j^*) = \begin{cases} 1 & \text{if the destination of a photon with direction r} \\ & \text{in the cell } (i^*, j^*) \text{ at time k is the cell } (i, j) \text{ at} \\ & \text{time } k+1 \text{ and its final direction of motion is s} \\ 0 & \text{in all the other cases} \end{cases}$$

The previous Eq. (9) gives the number of photons in the cell (i,j) at time k+1 with direction of motion s as the sum of all the photons in the cell of the neighbourhood with a given direction r which, moving in the cellular space, has the cell (i,j) as final destination and s as final direction of movement.

4.2 Electron-photon interaction and changes in the refractive index

The laser beam photons are travelling in a medium with variable refractive index. So, at each time step, it is necessary to evaluate the current photon direction and to accordingly change the photon state variable. Is worth stressing that, in the present model, this is the only situation in which a photon direction could be changed.

The refraction index modification is the consequence of the variable charge spatial distribution, due to electron movements. So, local gradients in the refractive index are obtained that modify the photon direction versor. The gradient of the refraction index $\nabla n_k(i,j)$ in each cell is computed by evaluating the local refraction index difference, i.e. the difference between the refraction index in the considered cell and the one in the cells of the neighbourhood. Once the local values for the refraction index have been computed the direction of the photons in each cell are modified according to the local value of the refraction index by computing the "force" acting on the photon and modifying its direction of propagation. This is done by modifying at each time step the matrix $R^{(r,s)}_{(k)}(i^*,j^*)$, where (i^*,j^*) indicates the cells belonging to the neighbourhood of the considered cell (i,j).

4.3 Electron-electron and the photon-electron interaction (Coulomb and ponderomotive forces)

In this cases there is no problem of direction of motion. In fact, the Coulomb and the ponderomotive forces, which determine the electron-electron-photon interaction, can act in all directions. So, the neighbourhood $\#$ is the set of the six nearest neighbour cells plus the considered cell.

The main problem in modelling interactions involving electrons is that once the forces acting on a single electron are known, they determine an acceleration through Newton's law, i.e. $a=F/m_e$, which produces changes in the velocity of the particles. In our model electrons are considered as "static", in the sense that they haven't any velocity state variable (they could be considered as having the same thermal velocity). Hence, the problem is how to describe the effect of forces in CA context with static electrons. In order to do this, we consider that the motion of one electron will be uniformly accelerated during the time step Δt and hence the electron displacement will be

$$\Delta x = \frac{1}{2}\frac{F}{m_e}(\Delta t)^2$$

Since in the model computation we always obtain $\Delta x << l$, i.e. a displacement less than the CA spatial step, we have displaced over l a number of electrons given by $\Delta x N_{el(0)}/l$, where $N_{el(0)}$ is the number of electrons initially present in the cell. The evolution rule, describing the dynamics of the electron number in each cell is given by:

$$N_{el(k+1)}(i,j) = N_{el(k)}(i,j) + \\ - \sum_{(i^*,j^*)\in\#(i,j)} \left[K_{1_{(k)}}^{(i^*,j^*)}(i,j) \left(\sum_{s=1}^{M} N_{ph_{(k)}}(i,j) - \sum_{s=1}^{M} N_{ph_{(k)}}(i^*,j^*) \right) \right] + \\ - \sum_{(i^*,j^*)\in\#(i,j)} \left[K_{2_{(k)}}^{(i^*,j^*)}(i,j) \left(N_{el(k)}(i,j) - N_i \right) \right] \qquad (10)$$

In the right side of the previous Eq. (10) three terms are evident:

- $N_{el(k)}(i,j)$, the number of electrons in the cell (i,j) at time k.
- $\sum_{(i^*,j^*)\in\#(i,j)} \left[K_{1_{(k)}}^{(i^*,j^*)}(i,j) \left(\sum_{s=1}^{M} N_{ph_{(k)}}(i,j) - \sum_{s=1}^{M} N_{ph_{(k)}}(i^*,j^*) \right) \right]$ represents the number of incoming (outgoing) electrons due to the effects of the ponderomotive force. This term is the sum of the contributions given by each cell of the neighbourhood. For each contribution, the number of moved electrons is proportional to the gradient of the optical field intensity, here represented by the difference between the total photon number in the considered cell and the total photon number in the currently considered cell of the neighbourhood.
- $\sum_{(i^*,j^*)\in\#(i,j)} \left[K_{2_{(k)}}^{(i^*,j^*)}(i,j) \left(N_{el(k)}(i,j) - N_i \right) \right]$ represents the number of incoming (outgoing) electrons due to the effects of the Coulomb force. Also in this case, this is the sum of the contributions given by each cell of the neighbourhood. The number of moved electrons is proportional to the net in the cells of the neighbourhood, i.e. the difference between the number of electron and the number of ions in each cell.

In Eq. (10) there are two constants to be tuned, namely $K_{1(k)}^{(i^*,j^*)}$ and $K_{2(k)}^{(i^*,j^*)}$. Note that the value of these constants can be both time-varying and space dependent. So, the number of electrons in the cell (i,j) at time k+1 is given by the number of electrons in the same cell at the previous time step modified by a quantity depending of the intensity of the Coulomb force and the ponderomotive force. The intensity of both the actions can be user-defined and eventually tuned on experimental data.

5 Simulation Results

In this section, simulation results obtained using the model described in the previous section will be presented using a step-by-step approach. In fact, results on the effects of each single evolution rule of the CA will be outlined separately, in order to check at each step the physical coherency of the obtained results.

5.1 Propagation of light through a focusing lens

First of all the propagation of photons in absence of matter has been studied, in order to verify if the proposed law (see Eq. (9)) allows to obtain focalization in geometric optics when the laser pulse passes through a thin lens. As already said the pulse is gaussian in space and time and has the following parameters: energy E = 10 mJ; pulse duration $\tau \cong$ 100 fs; input spot size $r_0 \cong 15$ μm.

If no diffractive effect is considered (geometrical optics framework), focalization of the pulse in a single point on the focal axis must be obtained. Then, after focusing, the pulse must widen again and, in absence of any perturbation, the starting situation should be reproduced on the opposite side of the CA. This is what has been obtained, but results of such simulations are not presented for the sake of brevity.

As a second step, similar simulations have been performed in the diffractive optics framework. In this case, it is expected the progressive decrease of the transversal dimensions of the laser pulse until it arrives at the focal plane, where its transverse dimension is minimum and equal to the focal spot size. In Fig. 3, the pulse is focused by a thin lens with parameter f/D = 7. It is worth noting that Fig. 3, and many others in the following, have been drawn using a technique typical of CA. The figure represents the CA (stretched to a matrix representation) and the value of the considered state variable is plotted in grey scale, the darker corresponding to a higher value of the state variable.

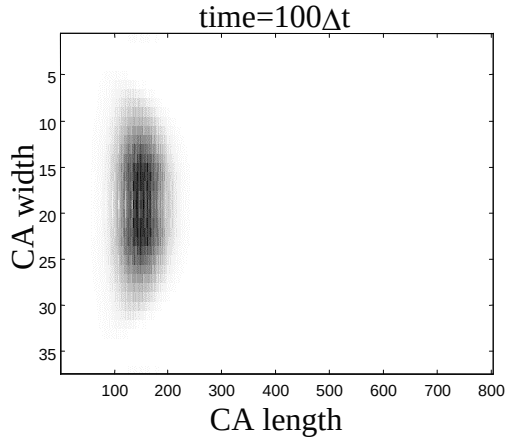

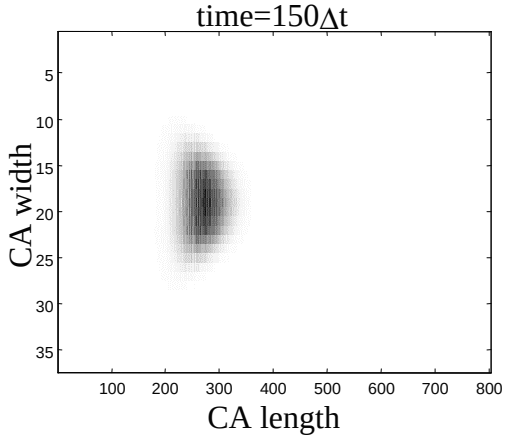

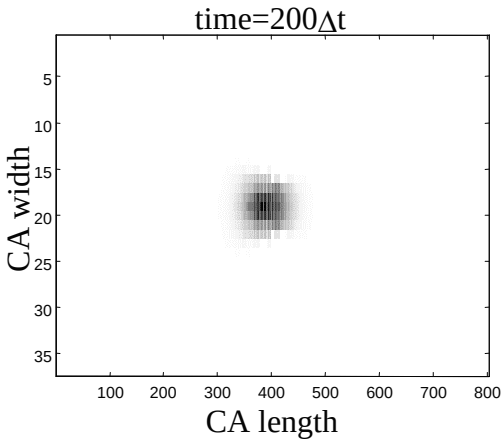

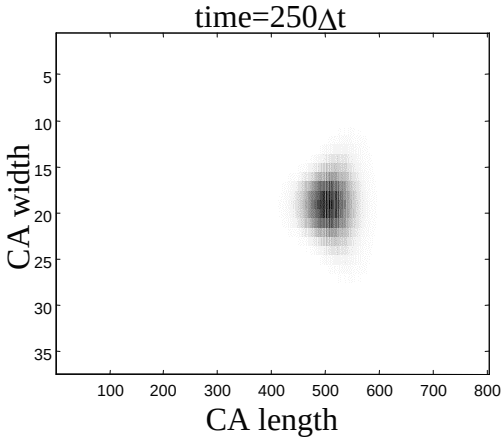

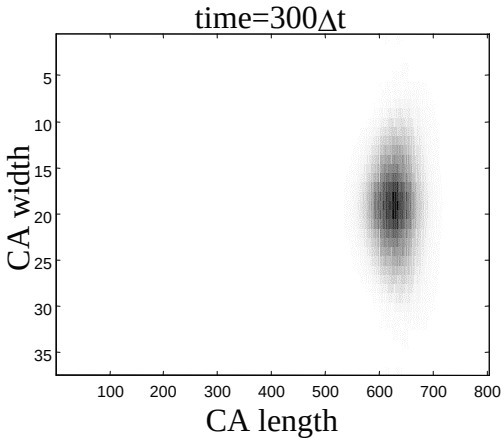

Figure 3: The laser pulse at different time, during its propagation in a vacuum region after focalisation by a thin lens. The figure is in grey scale, the darker corresponding to a higher number of photons. The CA spatial step is l = 1 μm; the each simulation time step is Δt = 3 fs.

The results in Fig. 3 allow the laser beam size to be measured as a function of time (space). The resulting trend is shown in Fig. 4, where the focal size is about 5 μm. The obtained trend can be compared with the analytical calculation for a gaussian laser beam, which is

$$R(z) = w_0 \left(1 + \left(\frac{Fz}{w_0^2} \right)^2 \right)^{\frac{1}{2}} \qquad (11)$$

where z=0 corresponds to the focal point; w_0 is the focal spot diameter and F=D/f is the f-number of the thin lens of diameter D. As already recalled, w_0 can be obtained by application of the Heisenberg principle, by noting that $w_0 \approx f\theta$ (with θ the angle under which the focal spot is seen by the lens) and $\theta \approx \Delta p/p \approx (h/D)/(h\nu/c) = \lambda/D$ (with h the Planck constant).

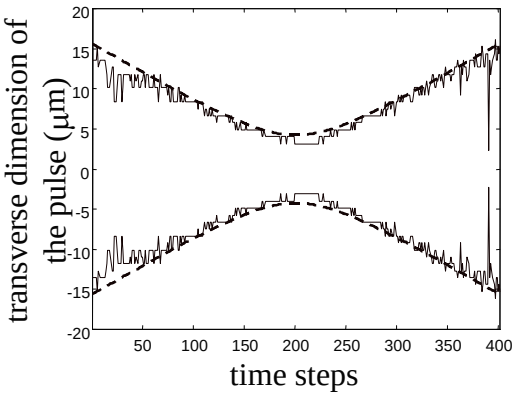

Figure 4: Width of the laser pulse (expressed in μm, wrt to the central axis of the CA) as a function of time (solid line). Theoretical prediction from diffractive optics (dotted line).

Numerical results compare very well with analytical predictions concerning both the focal spot size and the focal depth, i.e. the distance over which the variation in intensity is less than 10 % of the maximum value achieved at the focus.

5.2 Effect of ponderomotive force in absence of Coulomb interaction among electrons

In this section, the effects of ponderomotive force are introduced. In particular, it is supposed that it is the only force acting on the electrons, i.e. no coulombian interaction is active. This is equivalent to consider as a rule of evolution only the first two terms on the right hand of Eq. (10). So, electrons are forced to move away from their equilibrium position towards regions where the intensity of the optical field is smaller. This will happen with no reaction force provided by Coulomb electronic interaction.

In the following Fig. 5, temporal evolution of the system state variables (photon number and electron number) are plotted. After the passage of the laser pulse, an electron-free channel is obtained.

In Fig. 6 the obtained transversal modulation of electrons after the propagation of the beam in the region.

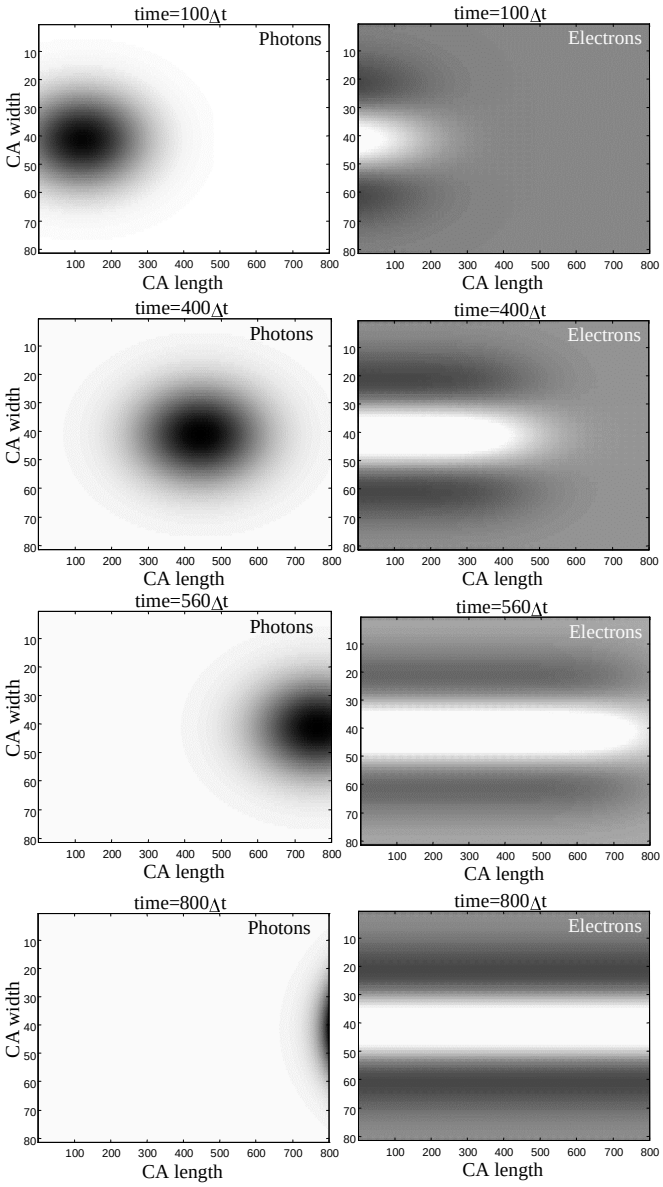

Figure 5: Photon number and electron number in grey scale (the darker, the higher the number) at different stages of time evolution of the simulation. The laser pulse propagates with a direction parallel to the system axis causing the movement of electrons in the areas where the intensity of the field is smaller. Since only ponderomotive force is considered and the refractive index of the medium is considered constant, no reaction due to charge displacement is visible.

The following physical parameters have been used in the simulation: l = 0.25 μm; Δt = 0.834 fs; refractive index n = 1; r_0 = 5 μm; $N_{el(0)}(i,j)=8 \times 10^7$ for all i,j. The pulse has been chosen with a peak amplitude of 9×10^{12} photons.

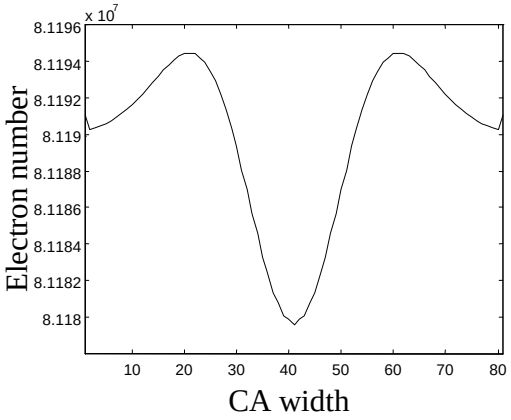

Figure 6: Electron number on a transversal section of the region filled with plasma after the passage of a laser pulse, considering only effects of ponderomotive force.

5.3 Beam propagation in a medium with constant refraction index

The passage of a laser pulse in a plasma causes the formation of a central channel with lower electron density, due to ponderomotive force, which moves electrons towards regions with smaller optical intensity. So, the electron density is no more uniform in the region filled with the plasma. Consequently, also the refractive index is not uniform in that region. In particular, if the Coulomb interaction is switched off, so as to say that in Eq. (10) the third term on the right hand side is zero, no other change in the electron density and in the refractive index will occur (since we have neglected hydrostatic pressure and thermal motion). Now, consider this "frozen time" situation and send into this region a second laser pulse. As a first approximation, it can be supposed that the refractive index of the region has a parabolic profile and so, the second laser pulse will travel through a region with constant refractive index due to a constant electron distribution.

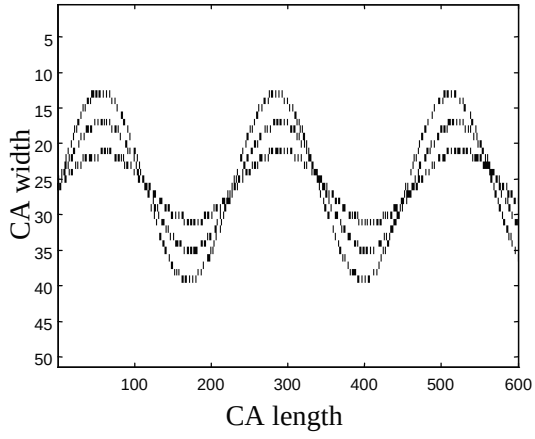

Figure 7: Propagation of light rays in the region filled with the plasma considered as a medium with parabolic refractive index for the effect of ponderomotive force.

In simulations, photons are introduced in the CA from the left side as rays of light with different incident angles. Rays have been simulated by using photon number profiles very narrow in space and with indefinite duration in time. Results of simulations are qualitatively and quantitatively similar those obtained using ray-optics theory. In Fig. 7, propagation of rays through the region is shown for different incident angles. The parameters used in the simulations are: maximum refraction index n_M=1.55; bulk refraction index n_b=1.4; parabolic profile from maximum to bulk is assumed; l = 1 μm; Δt = 10 fs.

Finally, it is worth noting that the propagation of photons in this plasma channel is exactly analogous to that in an optical fibre (in both cases the refractive index is higher on the central longitudinal axis).

5.4 Effects of Coulomb force reaction to the depletion due to ponderomotive force

When the radiation has completely crossed the region filled with plasma, an inhomogeneous distribution of charge is obtained (a transversal section can be seen in Fig. 6). So, an electric field will recall the electrons (positive ions are considered still) towards their equilibrium positions. Relaxation of electrons from the perturbed situation generated in the previous Sect 5.2 is obtained by effect of the electrical field generated by the charge spatial distribution. Plots of simulations are omitted for the sake of brevity. The physical parameters used are the same of the simulation of the previous Sect. 5.2. The final effect is simply a relaxation of the electron number in each cell to the initial value of $N_{el(0)}(i,j)=8 \times 10^7$. Only the simulation time step is different: here Δt = 1 ps. So, the process is about a thousand times slower than the depletion phenomenon caused by the laser pulse.

5.5 Coupled effects of ponderomotive force and refraction index changes: the self focusing

Finally, the rules of evolution of all the interactions are simultaneously considered. The coupled effects of ponderomotive force on electron distribution, the consequent modification of the refractive index and its effects on the optical propagation are described in Fig. 8, where a clear feedback is evident in the process dynamics.

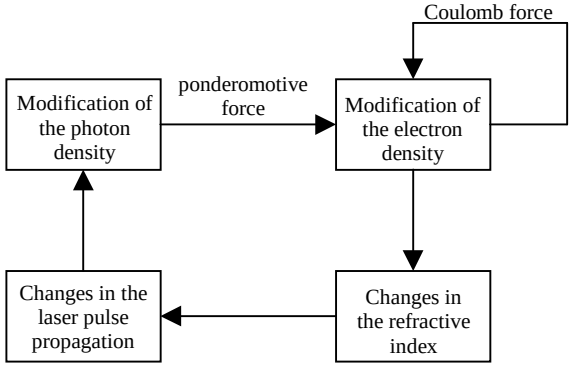

Figure 8: Schematic of laser-plasma interactions.

When an electromagnetic wave propagates in a hot plasma, electrons are forced to move towards regions where the intensity of the optical field is smaller, because of ponderomotive force. The obtained charge density gradient causes a coulombian recall field that moves electrons in the opposite direction (positive ions may be considered fixed). The local and instantaneous variation of the electric field causes a gradient of the refractive index, which influences the photon motion in plasma. The final effect of this process

is different depending on the power of the incoming laser pulse. In particular, if the power is sufficiently high (i.e. higher than the so called "critical power") the modification of the refraction index is so that the laser pulse is focalized in the material.

By considering all the interactions, simulations are provided showing the arising of self-focusing effects. In particular, Fig. 9.a shows the propagation of a laser pulse with power below the critical one. Fig. 9.b shows the self-focusing effect. The plots are obtained as three level plot of the electron number at increasing time. The chosen level are 30%, 60%, 90% of the peak number of photons.

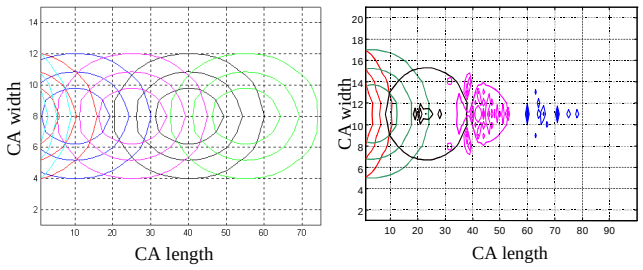

(a) **(b)**

Figure 9: Three level plots of the pulse during its propagation in the plasma taken every 20Δt (≅56fs). The ratio between the power of the laser pulse and the critical power is 0.33 in the first case (a) and 3 in the second (b).

The physical parameters of the incoming pulse are: E = 10 mJ; τ = 100 fs; r_0 = 5 μm; the critical power is P_{cr}=33 GW. The initial electron density in the plasma is $N_{el(0)}(i,j)=10^{22}$ for all i,j.

6 Discussion and Conclusions

As it is evident from the approach used in the presentation, the present work should be considered only as a preliminary one. However, this paper already shows the potentiality, as well as some limitations, of the CA approach to the simulation of laser-plasma interactions.

A first advantage of CA models is the insight they may give in the complex physical phenomena that are going on during the interactions. In the framework of CA models, the macroscopic physical effects simply arise from the "replication" of simple local and microscopic physical laws. In order to be more specific, first, we have been able to obtain good results, both qualitatively and quantitatively, concerning the propagation and focusing of the laser beam in free space and in a fixed density profile. This last point may be of interest also for the simulation of laser beam propagation in optical fibres. Secondly, we have been able to successfully describe the creation of a plasma channel due to ponderomotive forces. Results on self-focusing (again due to ponderomotive forces) of the laser beam in the plasma are instead for the moment only qualitative.

There are some limits connected either to our specific CA model or to CA in general. In the presented model we consider the electrons as "static", i.e. they may move from one cell to another but they are not characterised by a velocity. Hence, we cannot describe even simple phenomena such as plasma oscillations which are based on the transformation of (electric) potential energy in kinetic energy and vice versa. As a consequence, we are not able to describe also more complex phenomena, such as: the acceleration of electrons in the laser beam wake-field; the creation of electron currents and of the magnetic fields they produce (which may induce a pinching effect in the plasma); the variation of electron mass with velocity in the relativistic interaction regime. Since this last phenomenon is the origin of relativistic self-focusing, it follows that it cannot be fully modelled with our CA model.

Future work will be focused on introducing the electron velocity in this CA code. In principle, this is easy: it is sufficient to introduce many electron families, each characterised by its own velocity, in a similar way to what we have done with photon directions. However, in practice, this greatly increases the model complexity. In fact, the range of the electron velocity in the physical system is very large. The electron speed ranges from electron thermal velocity to light speed, for the electrons accelerated by the laser beams. Also, the thermal "slow" electrons and the "fast" ones have very different time constants and each of them must be dealt with sufficient resolution. On the other side, there are phenomena that are intrinsically difficult to be simulated with CA models, which are intrinsically "particle-based" codes. Indeed, in this context, the laser beam is described as a bunch of photons and it is difficult to consider the "wave-based" properties of an electromagnetic field. As a consequence, the generation of the electromagnetic fields (and even of magnetostatic fields connected to electron currents) is difficult to be described, as well as all long-range forces arising in the plasma as a consequence of the plasma dynamics itself. We recall again that in plasmas this is not the case of electrostatic (Coulomb) forces that are effectively screened over a distance of the order of the plasma Debye length. Hence, Coulomb forces in plasma are strictly short-range (local) and this makes their modelisation easy to obtain in a CA context.

The previous considerations fix an optimal range of laser and plasma parameters for which CA simulation of laser-plasma interactions can be performed and give physically sensible results. This is the regime of short pulse lasers at intermediate intensity (high, but non-relativistic) and moderate plasma density. This range is dominated by the effects of ponderomotive forces, while phenomena like electron acceleration and relativistic effects can reasonably be neglected.

Finally, another drawback of this modelling approach is the computation time, since the presented CA model have been simulated on single processor sequential computers. In fact, CA lend themselves naturally for parallel computer implementation, realizing a direct correspondence between the model structure (i.e. the cellular space topology) and the computation tool (i.e. the displacement of the processors in the machine). As an extreme consequence, it could be thought a direct one-to-one correspondence between the automaton cells and the computer processors. In future work, the problem of parallelizable algorithms will be also considered.

Acknowledgements

Paper supported by MURST Project "Identification and Control of Industrial Systems".

References

[1] Nisoli M., S. Stagira, S. De Silvestri, O. Svelto, S. Sartania, Z. Cheng, M. Lenzer, C. Spielmann, F. Krauss (1998). Compression of high energy femtosecond pulses by the hollow fiber technique: generation of sub-5 fs Multigigawatt pulses, in *Superstrong fields in plasmas*, M.Lontano, G.Mourou and F.Pegoraro Eds., American Institute of Physics, AIP Conf. Proc. 426, Woodbury, USA, pp. 304-313.

[2] Zepf M., J. Zhang, D. Chambers, A. Dangor, A. MacPhee, J. Lin, E. Wolfrum, J. Nilsen, T. Barbee, C. Danson, M. Key, C. Lewis, D. Neely, P. Norreys, S. Preston, R. O'Rourke, G. Pert, R. Smith, G. Tallents, I. Watts, J. Wark (1998). Recent progress in coherent XUV generation at RAL, in *Superstrong fields in plasmas*, M.Lontano, G.Mourou and F.Pegoraro Eds., American Institute of Physics, AIP Conf. Proc. 426, Woodbury, USA, pp. 499-508.

[3] Zepf M., G. Pretzler, U. Andiel, D. Chambers, A. Dangor, P. Norreys, J. Wark, I. Watts, G. Tsakiris (1998). Optimising harmonics from solid targets, in *Superstrong fields in plasmas*, M.Lontano, G.Mourou and F.Pegoraro Eds., American Institute of Physics, AIP Conf. Proc. 426, Woodbury, USA, pp. 264-269.

[4] Key M. (1999). Studies of the relativistic electron source and related phenomena in petawatt laser matter interactions, *Lawrence Livermore National Laboratory*, Report N. UCRL-JC-135477REV1, December.

[5] Dalla S., M. Lontano (1995). Excitation of large amplitude plasma waves by means of short and intense laser pulses, in *Non linear dynamic*, M. Costato and A. Degasperis Eds., Editrice Compositori, Bologna, Italy, pp. 211-218.

[6] Amiranoff F., V. Malka, D. Batani (1995). Non linear interactions in laser-plasmas, in *Non linear dynamic*, M. Costato and A. Degasperis Eds., Editrice Compositori, Bologna, Italy, pp. 119-126.

[7] Lontano M. (1995). Non linear effects in the propagation of electromagnetic waves in plasmas, in *Non linear dynamic*, M. Costato and A. Degasperis Eds., Editrice Compositori, Bologna, Italy, pp. 237-242.

[8] Batani D., A. Bernardinello, V. Masella, F. Pisani, M. Koenig, J. Krishnan, A. Benuzzi, S. Ellwi, T. Hall, P. Norreys, A. Djaoui, D. Nelly, S. Rose, P. Fews, M.Key (1998). Propagation in compressed matter of hot electrons created by short intense laser, in *Superstrong fields in plasmas*, M.Lontano, G.Mourou and F.Pegoraro Eds., American Institute of Physics, AIP Conf. Proc. 426, Woodbury, USA, pp. 372-376.

[9] Pukhov A., J. Meyer-ter-Vehn (1998). Relativistic non linear optics in plasmas by 3D PIC simulations, in *Superstrong fields in plasmas*, M.Lontano, G.Mourou and F.Pegoraro Eds., American Institute of Physics, AIP Conf. Proc. 426, Woodbury, USA, pp. 93-102.

[10] Ruhl H., F. Cornolti, F. Califano, A.Macchi (1998). Kinetic approach to superintense laser-solid interactions, in *Superstrong fields in plasmas*, M.Lontano, G.Mourou and F.Pegoraro Eds., American Institute of Physics, AIP Conf. Proc. 426, Woodbury, USA, pp. 282-287.

[11] Macchi A., F. Califano, F. Cornolti, B. Zambon, H.Ruhl (1998). Relativistic Maxwell-Boltzmann simulation of ultrashort, superintense laser-plasma interaction, in *Science and supercomputing at CINECA – Report '97* CINECA, Bologna Italy, pp. 522-529.

[12] Davies J., A. Bell, M. Haines, S.Guerin (1997). Short pulse high-intensity laser-generated fast electron transport into thick solids targets, *Physical Review E*, **56**, pp. 7193-7203.

[13] Toffoli T. (1984). Cellular Automata as an alternative to (rather than an approximation of) differential equations in modeling physics, in *Proceedings of an Interdisciplinary Workshop*, D.Farmer, T.Toffoli, S. Wolfram eds., North-Holland Physics Publishing.

[14] Frish U., B. Hasslacher, Y. Pomeau (1986). Lattice-Gas Automata for the Navier-Stokes Equation, *Phys. Rev. Lett.*, **56**, pp. 1500-1504.

[15] Bennet C. H., T. Toffoli, S. Wolfram (1986). *Cellular Automata 1986 Conference*. M.I.T. Press.

[16] Wolfram S. (1983). Statistical mechanics of Cellular Automata, *Rev. Mod. Phys.*, **55**, pp. 601-603.

[17] Bruschi M., P. M. Santini, O. Ragnisco (1992). Integrable Cellular Automata, *Phys. Lett. A*, **51**, p. 169.

[18] Cattaneo G., M. Milani, F. Magni, M. Rigotti (1996). A Cellular Automaton Model for Cooperative Effects in Matter Radiation Interaction: the Semiconductor Laser, *Il Nuovo Cimento*, **111B**, pp. 863-877.

[19] Dab D., J. P. Boon (1990). Cellular Automata Approach to Reaction-Diffusion Systems, in *Proceedings of an International Winter Workshop*, P. Manneville, N. Boccara, G. Y. Vichniac, R. Bidaux eds., Springer-Verlag.

[20] Doolen G. D. (1991). Lattice Gas Methods for PDE' s, Theory, Applications and Hardware, in *Proceedings of the NATO Advanced Research Workshop*, G.D. Doolen ed., Nort-Holland.

[21] Previdi F. (2000). A Stochastic Cellular Automaton for Modelling Radiation-Matter Interaction in Semiconductor Lasers, in *Proc. of MTNS2000*, Perpignan, France.

[22] Previdi F., M. Milani (1998). Cellular automaton approach to two-dimensional VCSEL array collective behaviour, *Il Nuovo Cimento*, **20D**, pp. 1625-1634.

[23] Burks C., D. Farmer (1984). Towards modelling DNA sequences as Automata, *Physica D*, **10**, pp. 157-167.

[24] Smith S.A., R.C. Watt, S.R. Hameroff (1984). Cellular Automata in cytoskeletal lattices, *Physica D*, **10**, pp. 168-174

[25] Di Gregorio S., R. Rongo, W. Spataro, G. Spezzano, D. Talia (1996). A parallel cellular tool for interactive modeling and simulation, *IEEE Computational Science and Engineering*, **3**, pp 33-43..

[26] Spezzano G., Talia D. (1998). Designing Parallel Models of Soil Contamination by the Carpet Language, *Future Generation Computer Systems*, North-Holland, **13**, pp. 291-302.

[27] Packard N. (1985). Lattice models for solidification and aggregation, in *Proc. of the 1st International Symposium for Science on Form*, Tsukuba, Japan.